Analysis of a Planar 3 Degree-Of-Freedom Adjustable Compliance Mechanism

Whee Kuk Kim*, Dong Gu Kim and Byung-Ju Yi*****

(Received June 24, 1995)

In this work, a planar three degree-of-freedom parallel mechanism as another type of assembly device which utilizes joint compliances is proposed. In order to generate the desired operational compliance characteristics at RCC point, these joint compliances can be adjusted either by properly replacing the joint compliances or by actively controlling stiffness at joints. The operational compliance matrix for this mechanism is obtained explicitly by symbolic manipulation, and its operational compliance characteristics are examined. It is found that the RCC point exists at the center of the workspace when the mechanism maintains symmetric configurations. Compliance characteristics and its sensitivity of this mechanism are analyzed with respect to the magnitude of the diagonal compliance components and two different matrix norms by measuring compliance sensitivity. It is expected that the analysis results provide the designer with a helpful information to determine a set of optimal parameters of this RCC mechanism.

Key Words: Joint Compliance, Parallel Mechanism, Remote Center Compliance (RCC) Mechanism, Sensitivity Analysis, Adjustable Compliance.

1. Introduction

Due to the limited precision of the position controlled robot manipulator system, one can not successfully perform insertion tasks requiring high precision such as electronic parts assembly tasks (e.g., peg-in-hole). Furthermore, imprecise position and/or orientation of the assembly bed, position sensor errors of the robots, non-uniformity of assembly parts, and non-rigidity of real bodies altogether hinders successful assembly operation. That is, they can increase the task completion time, and cause jamming or wedging during assembly operation quite often.

To cope with these problems, various control schemes have been investigated: force feedback control via Force/Torque sensor (Yi and Freeman, 1992; McCallion et al, 1980), compliance model based control (Cutkosky and Kao, 1989; Peshkin, 1990) for robot system and task environment, and compliance control using compliance devices such as Remote Center Compliance (RCC) devices (Whitney, 1986; Brussel, et al, 1986). These approaches can be categorized as active accommodation, passive accommodation, and passive-active accommotion (Whitney, 1987). Active accommodation method adjusts the robot position by utilizing force feedback signals to actively control the contact force occurring in contact with the task environment. Force control, damping control, impedance control, stiffness control, and vision sensor or proximity sensor based control belong to this method (Hogan, 1985; Kazerooni, et al., 1986). Passive accommodation method passively corrects the position error by utilizing the deformation of the compli-

* Department of Control and Instrumentation Engineering Korea University at Chochiwon, Seochang dong, Chochiwon, Yongi, Choong Nam, 339-800, Korea

** Robotics and Fluid Power Control Group, Korea Institute of Science and Technology, Cheongryang, Seoul, 130-650, Korea

*** Department of Control and Instrumentation Engineering Hanyang University at Ansan, Daehak dong, Ansan, Kyung-gi, 425-791, Korea

ant device attached to the wrist of the robot. Control methods using compliance devices, compliant work stations, air or gas stream, and magnetic force belong to this method. In general, when the passive compliance devices are used, the bandwidth and the stability of the system are increased, compared to the case when the active accommodation method is used. However, its position accuracy is decreased due to the use of compliant members as compared to the active accommodation method. Active-passive accommodation method combines the characteristics of the above two methods. Control methods using IRCC (Instrumented Remote Center of Compliance) which has both compliant members and Force/Torque sensor belong to this method. However, it is not cost-effective (De Fazio, et al., 1984).

In general, these RCC devices are made of linkages and compliant members such as elastomer shear pads, mechanical spring, rubber, or flexible members (Whitney, 1986). And its characteristics is represented as having a RCC point at which the operational compliance matrix is completely decoupled, and therefore when an external force or torque is applied to that point, the deformation occurs only along the direction of the applied force/torque. Optimal location of the RCC point in assembly tasks has not been theoretically established. However, Whitney showed experimentally that the position of RCC point should be located close to the contact point as much as possible to successfully complete assembly jobs without causing jamming or wedging (Whitney, 1982). Based on this part mating theory, most of compliance devices and RCC devices are implemented by attaching to the end of (wrist-type) robot. These RCC devices or compliance devices are used in tasks involving contacts with environment such as shaft insertion into bearing, rivet insertion into hole, bolt insertion into nut hole, and press fit and electronic part assembly tasks requiring high precision.

McCallion, et al. (1980) proposes a compliance device which uses the shape of Stewart platform mechanism that has been used as a flight simulator and a manipulator. They replace the six prismatic actuators by the same number of linear springs. However, the compliance matrix of this device is not completely diagonal (i.e., decoupled), and the position of the RCC point is not adjustable since it is fixed in the upper plate. Also, they proposed an improved RCC device (passive compliance devices) that uses three rigid prismatic links with the elastic membranes placed between the links and platforms. These elastic membranes represent 4 degrees-of-freedom compliance joints. Cutkosky implemented an actively adjustable RCC device that uses the hollow rubber spheres (Cutkosky and Wright, 1986). The location of the RCC point of the device is adjusted by controlling the hydraulic pressure inside the hollow rubber spheres.

Most of Commercial Remote Center Compliance (RCC) devices have been designed using deformable structures with constant magnitude of compliance. Therefore, their functionality as RCC device is very limited in that a certain job may require adjustable compliance characteristic during the assembly operation.

In this work, we propose a planar three degrees-of-freedom parallel mechanism (Fig. 1) as another type of assembly device which utilized joint compliances. In order to generate a desired operational compliance characteristic at RCC point, these joint compliances can be adjusted either by properly replacing the joint compliances or by actively controlling stiffness at joints.

2. Compliance Characteristics of a Planar 3-DOF Parallel Mechanism

The proposed mechanism in this paper consists of a floating ternary link, a base, three serial sub-chains, and a joint compliance at each base joint, as shown in Fig. 1. Each of sub-chain possesses three revolute joints connecting two adjacent links.

$_r\phi_n$ denotes the joint angle of nth joint in the r th subchain and $_rl_n$ denotes the link length of the nth link in the rth subchain. Also, let the output position/orientation vector representing the center of the upper platform be $\boldsymbol{u}=(x\ y\ \phi)^T$, and let

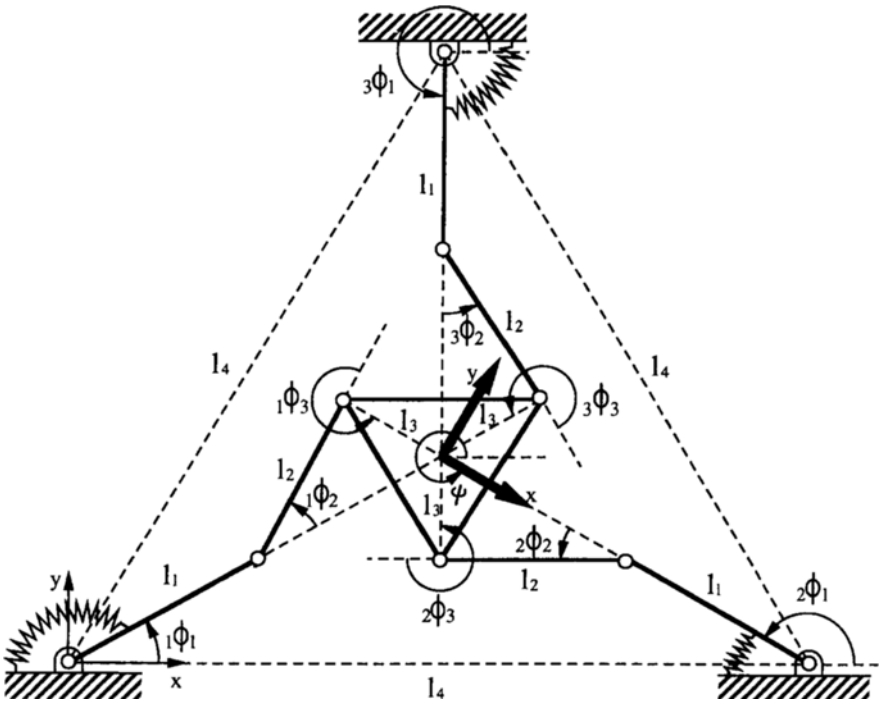

Fig. 1 A Planar 3-Degree-of-Freedom RCC Mechanism

the joint angles of the rth serial subchain be ${}_r\boldsymbol{\phi}=({}_r\phi_1\ {}_r\phi_2\ {}_r\phi_3)^T$. Then the differential relation between these two vectors is represented as

$$\boldsymbol{\delta u}=[{}_rG_\phi^u]\boldsymbol{\delta}_r\phi,\ r=1,2,3 \tag{1}$$

Assuming that Jacobian ($[{}_rG_\phi^u]$) of each serial subchain is non-singular, the inverse relation of Eq. (1) is given as

$$\boldsymbol{\delta}_r\boldsymbol{\phi}=[{}_rG_\phi^u]^{-1}\boldsymbol{\delta u},\ r=1,2,3 \tag{2}$$

From this equation, the differential relation between the input joint variables which consist of the base joints of three serial subchains $\boldsymbol{\phi}_a=({}_1\phi_1\ {}_2\phi_1\ {}_3\phi_1)^T$, and the output variables $\boldsymbol{u}=(x\ y\ \phi)^T$ can be obtained as (Yi and Freeman, 1992)

$$\boldsymbol{\delta}\phi_a=[G_u^a]\boldsymbol{\delta u} \tag{3}$$

where

$$[G_u^a]=\begin{bmatrix}[{}_1G_\phi^u]_{1,}^{-1}\\ [{}_2G_\phi^u]_{1,}^{-1}\\ [{}_3G_\phi^u]_{1,}^{-1}\end{bmatrix} \tag{4}$$

where $[{}_1G_\phi^u]_{i,}^{-1}$ denotes all the ith row elements of $[{}_1G_\phi^u]^{-1}$. Especially, when the nth link lengths of three serial subchains are the same (i.e., ${}_1l_n={}_2l_n={}_3l_n$, for $n=1,2,3$) Jacobian $[G_u^a]$ can be obtained explicitly as

$$[G_u^a]=\begin{bmatrix}\dfrac{C_{12}^1}{l_1S_2^1} & \dfrac{S_{12}^1}{l_1S_2^1} & \dfrac{l_3S_3^1}{l_1S_2^1}\\ \dfrac{C_{12}^2}{l_1S_2^2} & \dfrac{S_{12}^2}{l_1S_2^2} & \dfrac{l_3S_3^2}{l_1S_2^2}\\ \dfrac{C_{12}^3}{l_1S_2^3} & \dfrac{S_{12}^3}{l_1S_2^3} & \dfrac{l_3S_3^3}{l_1S_2^3}\end{bmatrix} \tag{5}$$

where C_{12}^1 implies $Cos({}_1\phi_1+{}_1\phi_2)$, and so on. Then the inverse relation of Eq. (3) is given as

$$\boldsymbol{\delta u}=[G_u^a]^{-1}\boldsymbol{\delta}\phi_a=[G_a^u]\boldsymbol{\delta}\phi_a \tag{6}$$

Let $\boldsymbol{\tau}=(\tau_1\ \tau_2\ \cdots\ \tau_n)^T$ and $\boldsymbol{f}=(f_1\ f_2\ \cdots\ f_m)^T$ be an actuator torque vector and an external force vector applied to the RCC point, respectively. Then from the virtual work's principle, the following equation holds:

$$\boldsymbol{d}\phi_a{}^T\boldsymbol{\tau}=\boldsymbol{d}u^T\boldsymbol{f} \tag{7}$$

Inserting Eq. (6) into Eq. (7) yields

$$\boldsymbol{\tau}=[G_a^u]^T\boldsymbol{f} \tag{8}$$

When the joint compliances at the input joints $\boldsymbol{\phi}_a=({}_1\phi_1\ {}_2\phi_1\ {}_3\phi_1)^T$ is represented as $C_{\phi 1}$, $C_{\phi 2}$, $C_{\phi 3}$ respectively, and the relation between $\delta\phi_{ai}$ and τ_i

at each joint is given as,

$$\delta\phi_{ai}=C_{\phi i}\tau_i \tag{9}$$

the relation between the inputs and the outputs can be represented, in a matrix form, as

$$\boldsymbol{\delta\phi}_a=[C_{\phi\phi}]\boldsymbol{\tau} \tag{10}$$

where the joint compliance matrix is expressed as

$$[C_{\phi\phi}]=\begin{bmatrix} C_{\phi 1} & 0 & 0 \\ 0 & C_{\phi 2} & 0 \\ 0 & 0 & C_{\phi 3} \end{bmatrix} \tag{11}$$

From Eqs. (6), (8) and (10), we have

$$\begin{aligned}\boldsymbol{\delta u}&=[G_a^u]\boldsymbol{\delta\phi}_a\\ &=[G_a^u][C_{\phi\phi}]\boldsymbol{\tau}\\ &=[G_a^u][C_{\phi\phi}][G_a^u]^T\boldsymbol{f}\\ &=[C_{uu}]\boldsymbol{f}\end{aligned} \tag{12}$$

where the operational compliance matrix $[C_{uu}]$ is defined as

$$[C_{uu}]=[G_a^u]\,[C_{\phi\phi}][G_a^u]^T \tag{13}$$

or noting that the following relations hold,

$$[K_{uu}]=[C_{uu}]^{-1} \tag{14}$$

$$[K_{\phi\phi}]=[C_{\phi\phi}]^{-1} \tag{15}$$

the stiffness matrix can be represented as

$$[K_{uu}]=([G_a^u][K_{\phi\phi}]^{-1}[G_a^u]^T)^{-1} \tag{16}$$

In order for this operational compliance matrix to be symmetric, the off-diagonal elements should be zero. And these conditions can be written by a matrix form as

$$\begin{bmatrix} C_{xy} \\ C_{x\psi} \\ C_{y\psi} \end{bmatrix}=\begin{bmatrix} A_{11} & A_{12} & A_{13} \\ A_{21} & A_{22} & A_{23} \\ A_{32} & A_{32} & A_{33} \end{bmatrix}\begin{bmatrix} C_{\phi 1} \\ C_{\phi 2} \\ C_{\phi 3} \end{bmatrix}=\begin{bmatrix} 0 \\ 0 \\ 0 \end{bmatrix} \tag{17}$$

where

$$A_{11}=l_3l_1^2(S_2^1)^2(C_{12}^3S_3^2-C_{12}^2S_3^3)(S_{12}^2S_3^3-S_3^2\,S_{12}^3) \tag{18}$$

$$A_{12}=l_3l_1^2\,(S_2^2)^2(S_3^1S_{12}^3-S_{12}^1S_3^3)(C_{12}^1\,S_3^3-S_3^1C_{12}^3) \tag{19}$$

$$A_{13}=l_3l_1^2(S_2^3)^2(S_{12}^1S_3^2-S_3^1S_{12}^2)(S_3^1C_{12}^2-C_{12}^1S_3^2) \tag{20}$$

$$A_{21}=l_1^2l_3(S_2^1)^2(C_{12}^2S_{12}^3-C_{12}^3S_{12}^2)(S_{12}^2S_3^3-S_3^2S_{12}^3) \tag{21}$$

$$A_{22}=l_1^2l_3(S_2^2)^2(C_{12}^3S_{12}^1-C_{12}^1S_{12}^3)(S_3^1S_{12}^3-S_{12}^1S_3^3) \tag{22}$$

$$A_{23}=l_1^3l_3(S_2^3)^2(S_{12}^2C_{12}^1-C_{12}^2S_{12}^1)(S_{12}^1S_3^2-S_3^1S_{12}^2) \tag{23}$$

$$A_{31}=l_1^2l_3(S_2^1)^2(C_{12}^2S_{12}^3-C_{12}^3S_{12}^2)(C_{12}^3S_3^2-C_{12}^2S_3^3) \tag{24}$$

$$A_{32}=l_1^2l_3(S_2^2)^2(C_{12}^3S_{12}^1-C_{12}^1S_{12}^3)(C_{12}^1S_3^3-C_{12}^3S_3^1) \tag{25}$$

$$A_{33}=l_1^2l_3(S_2^3)^2(C_{12}^1S_{12}^2-C_{12}^2S_{12}^1)(C_{12}^2S_3^1-C_{12}^1S_3^2) \tag{26}$$

The condition for Eq. (17) to have a non-trivial solution is that the determinant of the matrix A should be zero. This condition can be satisfied especially when the symmetric configuration of the system is maintained and the joint compliances attached to the three base joints are the same; that is,

$$\begin{aligned}&{}_2\phi_1={}_1\phi_1+\frac{2}{3}\pi,\ {}_3\phi_1={}_1\phi_1+\frac{4}{3}\pi\\ &{}_1\phi_2={}_2\phi_2={}_3\phi_2,\ {}_1\phi_3={}_2\phi_3={}_3\phi_3\\ &C_\phi=C_{\phi 1}=C_{\phi 2}=C_{\phi 3}\end{aligned} \tag{27}$$

In this case, the diagonal components of the output compliance matrix are given as

$$C_{xx}=\frac{2C_\phi l_1^2(S_2^1)^2}{3} \tag{28}$$

$$C_{yy}=\frac{2C_\phi l_1^2(S_2^1)^2}{3} \tag{29}$$

$$C_{\psi\psi}=\frac{C_\phi l_1^2(S_2^1)^2}{3l_3(S_3^1)^2} \tag{30}$$

It can be observed from Eqs. (28)~(30) that the magnitudes of the diagonal components of the operational compliance matrix are functions of the joint compliance, the link lengths, and the joint angles, and that the following two conditions hold

$$C_{xx}=C_{yy} \tag{31}$$

$$\frac{C_{xx}}{C_{\psi\psi}}=\frac{l_3(S_3^1)^2}{2} \tag{32}$$

Note that the magnitude-ratio of the translational component to the rotational component of the operational compliance matrix is related by link length l_3 and the angular displacement ϕ_3^1.

A most desirable property of a RCC device is having a low compliance sensitivity about its RCC point. In the following section, the sensitivity matrix for the compliance matrix is derived and sensitivity analysis is performed.

3. Sensitivity Analysis

To assure one of excellent RCC characteristics such as low sensitivity of the compliance matrix, the sensitivity analysis of the operational compliance matrix is required. The compliance sensitivity matrix of the mechanism can be derived by taking partial derivative of $[C_{uu}]$ with respect to output variables $\boldsymbol{u}$, as

$$\frac{\partial[C_{uu}]}{\partial \boldsymbol{u}}=\left[\frac{\partial[C_{uu}]}{\partial u_1}\ \frac{\partial[C_{uu}]}{\partial u_2}\ \cdots\ \frac{\partial[C_{uu}]}{\partial u_n}\right] \tag{33}$$

where the output $\boldsymbol{u}=(u_1\ u_2\ \cdots\ u_m)^T$ is a $m\times 1$ vector and the input $\boldsymbol{\phi}=(\phi_1\ \phi_2\ \cdots\ \phi_n)^T$ is a $n\times 1$ vector. Noting that $[C_{uu}]$ is a $m\times m$ matrix, $\frac{\partial[C_{uu}]}{\partial \boldsymbol{u}}$ is a $m\times(m\times m)$ 3-dimensional matrix, where $\frac{\partial[C_{uu}]}{\partial u_i}$ is a $m\times m$ matrix and represents the ith plane of the compliance sensitivity matrix. Also, noting that $[C_{uu}]$ is a function of joint variables ($\boldsymbol{\phi}$) as shown in Eq. (13), the $(m,\ n)$ element of the ith plane matrix $\left(\frac{\partial[C_{uu}]}{\partial u_i}\right)$ can be obtained by using a chain rule as follows

$$\frac{\partial[C_{uu}]_{m:n}}{\partial u_i}=\left(\frac{\partial\phi_1}{\partial u_i}\ \frac{\partial\phi_2}{\partial u_i}\ \cdots\ \frac{\partial\phi_n}{\partial u_i}\right)\cdot\begin{bmatrix}\frac{[C_{uu}]_{m:n}}{\partial\phi_1}\\ \frac{\partial[C_{uu}]_{m:n}}{\partial\phi_2}\\ \cdots\\ \frac{\partial[C_{uu}]_{m:n}}{\partial\phi_n}\end{bmatrix} \tag{34}$$

Then, the partial derivative of the compliance matrix with respect to u_i can be represented, in a simple form, as

$$\frac{\partial[C_{uu}]}{\partial u_i}=\left(\frac{\partial\boldsymbol{\phi}}{\partial u_i}\right)^T\cdot\left[\frac{\partial[C_{uu}]}{\partial\boldsymbol{\phi}}\right] \tag{35}$$

where $\frac{\partial[C_{uu}]}{\partial\boldsymbol{\phi}}$ is defined as

$$\frac{\partial[C_{uu}]}{\partial\boldsymbol{\phi}}=\left[\frac{\partial[C_{uu}]}{\partial\phi_1}\ \frac{\partial[C_{uu}]}{\partial\phi_2}\ \cdots\ \frac{\partial[C_{uu}]}{\partial\phi_n}\right] \tag{36}$$

This 3-dimensional sensitivity matrix is arranged so that the matrix $\left[\frac{\partial[C_{uu}]}{\partial\phi_i}\right]$ represents the ith plane. The operator ($\cdot$), called as a generalized dot product, is used as an operator performing dot operation between the row vector $\left(\frac{\partial\boldsymbol{\phi}}{\partial u_i}\right)^T$ and the plane vector $\frac{\partial[C_{uu}]_{m:n}}{\partial\boldsymbol{\phi}}$ which is formed with $(m,\ n)$ elements of each plane $\left[\frac{\partial[C_{uu}]}{\partial\phi_i}\right]$. Thus, the whole 3-dimensional sensitivity matrix can be written as the following form

$$\frac{\partial[C_{uu}]}{\partial\boldsymbol{u}}=\begin{bmatrix}\left(\frac{\partial\boldsymbol{\phi}}{\partial u_1}\right)^T\cdot\left[\frac{\partial[C_{uu}]}{\partial\boldsymbol{\phi}}\right]\\ \left(\frac{\partial\boldsymbol{\phi}}{\partial u_2}\right)^T\cdot\left[\frac{\partial[C_{uu}]}{\partial\boldsymbol{\phi}}\right]\\ \cdots\\ \left(\frac{\partial\boldsymbol{\phi}}{\partial u_m}\right)^T\cdot\left[\frac{\partial[C_{uu}]}{\partial\boldsymbol{\phi}}\right]\end{bmatrix}=[G_u^{\phi}]^T\cdot\left[\frac{\partial[C_{uu}]}{\partial\boldsymbol{\phi}}\right] \tag{37}$$

Using Eq. (13), Eq. (37) can be rewritten as

$$\frac{\partial[C_{uu}]}{\partial\boldsymbol{u}}=[G_u^{\phi}]^T\cdot\left[\frac{\partial[G_{\phi}^u]}{\partial\boldsymbol{\phi}}[C_{\phi\phi}][G_{\phi}^u]^T+[G_{\phi}^u][C_{\phi\phi}]\frac{\partial[G_{\phi}^u]^T}{\partial\boldsymbol{\phi}}\right] \tag{38}$$

See Appendix for the method of obtaining $\frac{\partial[G_{\phi}^u]}{\partial\boldsymbol{\phi}}$ indirectly via the second-order kinematic influent coefficients $[H_{\phi\phi}^u]$ (Freeman and Tesar, 1988).

The desirable properties of RCC device are low and uniform sensitivity of the compliance matrix at RCC point. Noting that the compliance sensitivity matrix is 3-dimensional, the Frobenius norm or the 2-norm of each plane compliance matrix can be employed to find the optimal parameters of the device. The Frobenius norm of the matrix A is defined as the square root of the sum of the absolute-square magnitude of all the matrix elements, and is given as

$$\|A\|_F=\left(\sum_{i=1}^{m}\sum_{j=1}^{n}|a_{ij}|^2\right)^{\frac{1}{2}}\ \forall A\in C^{m\times n} \tag{39}$$

where a_{ij} denotes the ith row and the jth column element of the matrix A. The 2-norm of the matrix A is defined as

$$\|A\|_2=\sup_{x\neq 0,\ x\in C^n}\frac{\|A\boldsymbol{x}\|_2}{\|\boldsymbol{x}\|_2}\ \forall A\in C^{m\times n} \tag{40}$$

and can be also obtained as

$$\|A\|_2=\bar{\sigma}(A) \tag{41}$$

where $\bar{\sigma}(A)$ represents the maximum singular value of A. Note that these two norms are equivalent norms from the following relation

$$\|A\|_2\leq\|A\|_F\leq\sqrt{n}\,\|A\|_2 \tag{42}$$

Although any of the two matrix norms can be employed in the analysis of operational compliance sensitivity, the concept of 2-norm is em-

ployed in the following sensitivity analysis.

The largest singular value of $\frac{\partial[C_{uu}]}{\partial u_i}$ implies the largest deviation from the current compliance characteristic. Therefore, the largest singular value of the sensitivity plane matrices $\frac{\partial[C_{uu}]}{\partial u_i}$ for $i = 1,2, \cdots, m$ can be used as the measure of compliance sensitivity. It will be denoted as s_{max}.

On the other hand, in order to obtain the characteristics of uniform compliance sensitivity along any direction, the average of the largest singular values of each sensitivity plane matrix $\frac{\partial[C_{uu}]}{\partial u_i}$ for $i=1,2, \cdots, m$ can also be used as another measure of compliance sensitivity. It will be denoted as s_{avg}. Furthermore, compliance sensitivity norm can be obtained by providing different weights to the largest singular values of each plane of compliance sensitivity matrices, depending on task requirements. However, in this paper, we consider the case of the same weight.

In the following plots, we call the former norm as "largest 2-norm" and the latter norm as "mean 2-norm", for convenience. These two criteria will be used in the analysis of operational compliance.

4. Analysis of Operational Compliance

It is shown that when the three degrees-of-freedom mechanism maintains a symmetric configuration, a RCC point exists at the center of the mechanism. Without loss of generality, the three base joints of the mechanism are located at the corners of the equilateral triangle with its lateral length l_4, as shown in Fig. 1. When the distance from the base joint to the center point of the mechanism is set to 1, it can be shown from the symmetric geometry that the lateral length l_4 of the equilateral triangle is equal to $\sqrt{3}$. Also, the position of RCC point with respect to the base coordinate system shown in Fig. 1 is obtained as

$$x=\frac{l_4}{2}=\frac{\sqrt{3}}{2},\ y=\frac{l_4}{2\sqrt{3}}=\frac{1}{2} \tag{43}$$

Symmetric configuration of the RCC mechanism is decided by four parameters (l_1, l_2, l_3, ψ) with the x, y positions of the floating ternary link fixed. In simulations, we investigated the cases of five different values of l_1 (i.e., l_1=0.3, 0.6, 0.9, 1.2, 1.5). However, since the results from different values of l_1 shows very similar trends as those of the other cases, in the following, we only discussed the case that the first link length l_1 of each serial subchain equals to 0.9 . For each of three different output orientation angles ($\psi=-30^o$, 0^o, 30^o), we will examine the characteristics of both the two compliance components ($C_{xx}=C_{yy}$, $C_{\psi\psi}$) and the two different norms (i.e., s_{max} and s_{avg}) of the compliance sensitivity matrix, at the RCC point by varying the link lengths, l_2 and l_3.

Figures. 2~5, 6~9, and 10~13 represent the contour plots of two different norms for compliance sensitivity and those of C_{xx} and $C_{\psi\psi}$ for the fixed orientation angles, $\psi=-30^o$, 0^o, 30^o,

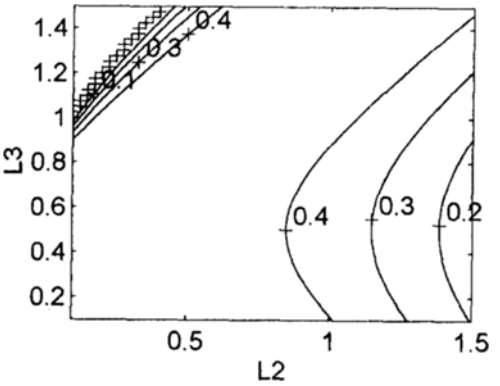

Fig. 2 Compliance Plot $C_{xx}=C_{yy}$: l_1=0.9, $\psi=-30^o$

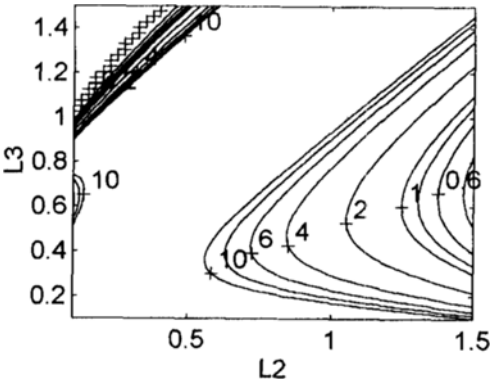

Fig. 3 Compliance plot $C_{\psi\psi}$: l_1=0.9, $\psi=-30^o$

respectively, under the assumption of unit magnitude of the compliance at each base joint. The maximum threshold value of the norms for both compliances and compliances sensitivity is set to be 10 and the minimum threshold value of the norms is set to be 0.1, respectively, for convenience. Thus, the norm values greater than 10 or less than 0.1 are not shown in the plots.

From Figs. 2~5 and Figs. 10~13, it can be observed that as the magnitudes of both the orientation component and translational component of the operational compliance matrix increase, the magnitude of compliance sensitivity tends to increase. However, from Figs. 6~9, it can be observed that as the magnitude of the orientation component of the operational compliance matrix increases, the magnitude of compliance sensitivity tends to increase, while the characteristic of the translational components of the operational compliance matrix is not coincident to the one of the compliance sensitivity. This different trend in Fig. 6~9 can be easily seen by observing that magnitude of $C_{\phi\phi}$ is varied more rapidly then that of C_{xx} with respect to the variation of link lengths l_2 and l_3.

From all these plots, it can also be noted that two different sensitivity norms (s_{max} and s_{avg}) show a similar trend, and that as the design parameters get close to the singular configuration (or unreachable configuration : marked lines by cross), the magnitudes of norms for compliances rapidly decrease, but the magnitudes of the norms for compliance sensitivity rapidly increase.

In the design of RCC mechanism, one of the design objectives is to obtain a completely decoupled compliance matrix and a various magnitude

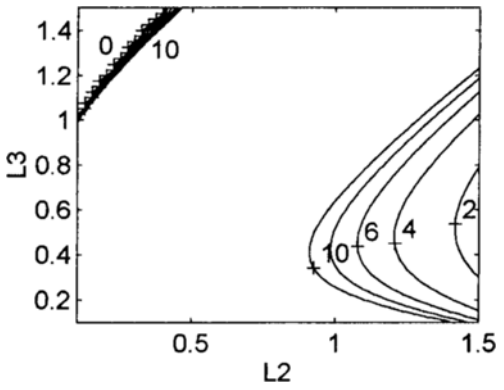

Fig. 4 Largest 2-Norm of Compliance sensitivity (s_{max}): $l_1=0.9$, $\psi=-30^o$

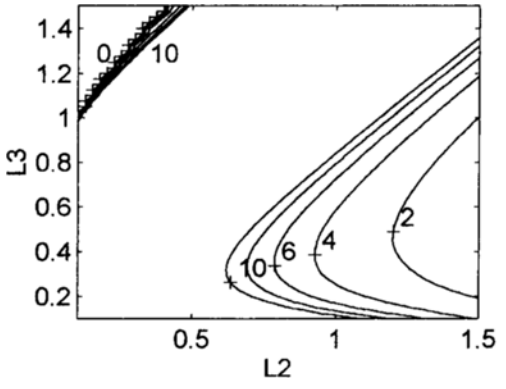

Fig. 5 Mean 2-Norm of Compliance Sensitivity (s_{avg}): $l_1=0.9$, $\psi=-30^o$

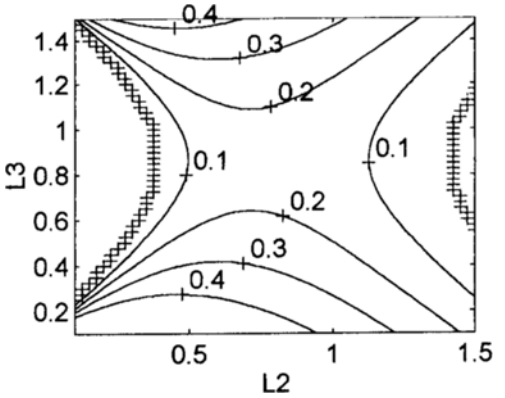

Fig. 6 Compliance Plot $C_{xx}=C_{yy}$: $l_1=0.9$, $\psi=0^o$

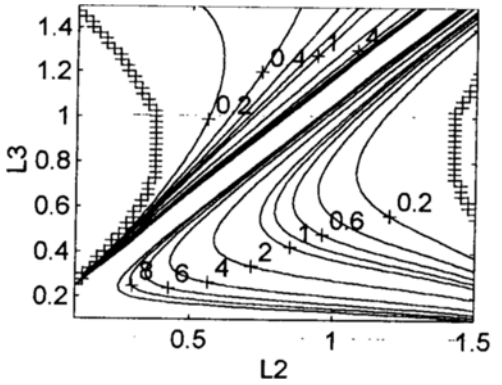

Fig. 7 Compliance plot $C_{\phi\phi}$: $l_1=0.9$, $\psi=0^o$

of diagonal compliance components with small and uniform sensitivity of compliance components. However, from the above analysis it is shown that there exists some trade-off between compliance and its sensitivity. Therefore, when the magnitude of the desired operational compli-

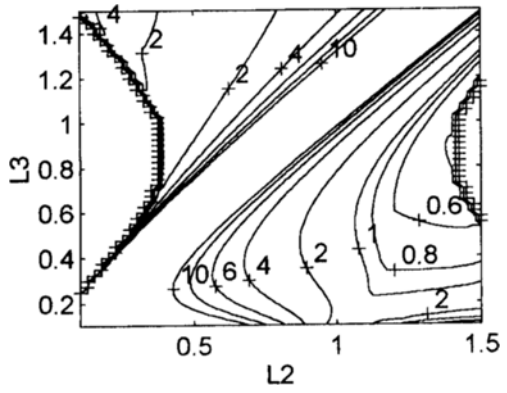

Fig. 8 Largest 2-Norm of Compliance sensitivity (s_{max}): $l_1=0.9$, $\psi=0^o$

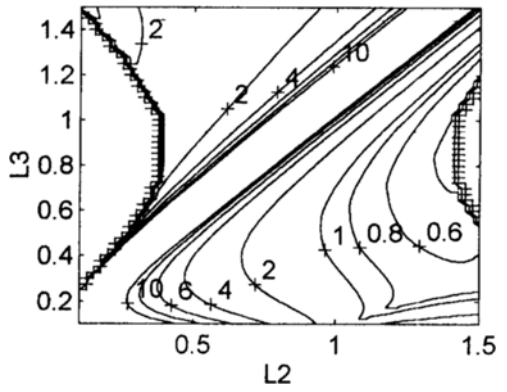

Fig. 9 Mean 2-Norm of Compliance Sensitivity (s_{avg}): $l_1=0.9$, $\psi=0^o$

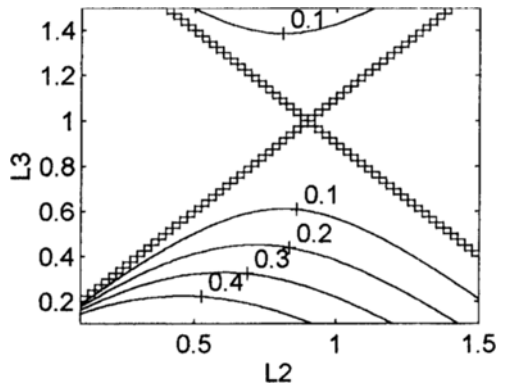

Fig. 10 Compliance Plot $C_{xx}=C_{yy}$: $l_1=0.9$, $\psi=30^o$

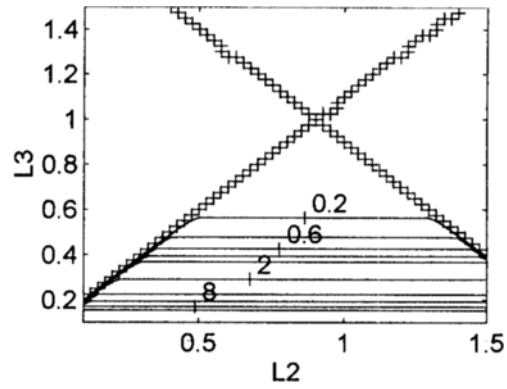

Fig. 11 Compliance plot $C_{\psi\psi}$: $l_1=0.9$, $\psi=30^o$

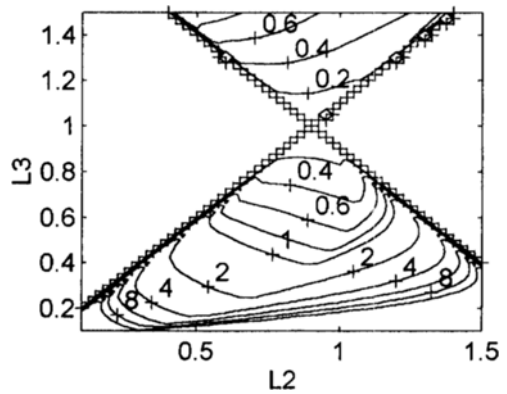

Fig. 12 Largest 2-Norm of Compliance sensitivity (s_{max}): $l_1=0.9$, $\psi=30^o$

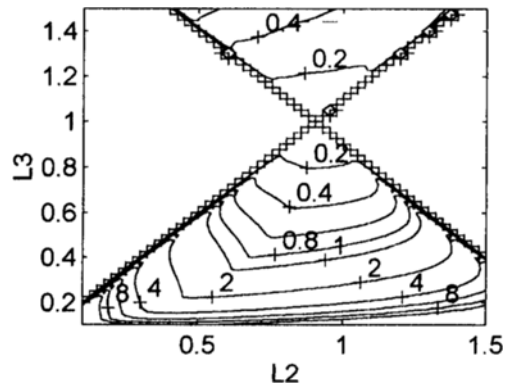

Fig. 13 Mean 2-Norm of Compliance Sensitivity (s_{avg}): $l_1=0.9$, $\psi=30^o$

ance components and the tolerance level of compliance sensitivity are given, these plots can be used to identify optimal link lengths and optimal orientation angle of this mechanism.

Note, however, that in this study we only considered the cases for five different fixed values of l_1's(0.3, 0.6, 0.9, 1.2, 1.5) and only three different fixed output orientation angles ($\phi = -30^o$, 0^o, 30^o). As an alternative way, a set of optimal parameters can be obtained in a systematic manner by defining a cost function which simultaneously represents the characteristics of compliance and its tolerable sensitivity.

In the implementation of the joint compliance, several types can be considered. To obtain a passive compliance effect, a passive coil spring, a rubber, a joint member with a neck-down section, etc. can be employed. However, since the compliance of this kinds of passive type is not adjustable, a compliance effect which can be actively generated and adjusted is preferred. This effect can be effectively obtained by using pneumatic type of actuator in which the inner pressure of the cylinder is controllable.

5. Conclusion

In this paper, compliance characteristics of a planar parallel 3-degrees-of-freedom mechanism using only minimum set of joint compliances are investigated. It is found that a RCC point exists at the center of the mechanism when it maintains symmetric configurations, and that its compliance characteristics at the RCC point can be adjusted by varying link lengths, joint compliances and its orientation.

Compliance characteristics and its sensitivity of this mechanism are analyzed with respect to the magnitude of the diagonal compliance component and two different matrix norms by measuring compliance sensitivity. It is believed that the simulation results can provide the designer with a helpful information to determine a set of optimal parameters for this type of RCC mechanisms.

As future works, we can investigate the compliance characteristics, when placing the compliances at different joints of the mechanism besides the base joints, when placing compliant member at more joints than the system's degree of freedom and when imposing antagonistic preloading between the joints (Yi and Freeman, 1992).

Acknowledgment

This research is supported by Korea Science and Engineering Foundation (No: 951-1008-079-2). The support of the KOSEF is greatly appreciated.

References

Brussel, H. V. Thielemans, H. and Simons, J., 1986, "Further Developments of The Active Adaptive Compliant Wrist (AACW) For Robot Assembly," *Proc. th Int'l Symp. on Industrial Robots, SME*, pp. 377~384.

Cutkosky, M. R. and Wright, P. K., 1986, "Active Control of a Compliant Wrist in Manufacturing Tasks," *Transactions of the ASME*, Vol. 108, pp. 36~43.

Cutkosky, M. R. and Kao, Imin, 1989, "Computing and Controlling the Compliance of a Robotic Hand," *IEEE transaction. of robotics and automation*, Vol. 5, No. 2, pp. 151~165.

De Fazio, T. L., Seltzer, D. S. and Whitney, D. E., 1984, "The Instrumented Remote Center Compliance," *The Industrial Robot*, Vol. 11, No. 4, pp. 238~242.

Freeman R. A. and Tesar, D., 1988, "Dynamic Modeling of Serial and Parallel Mechanisms/ Robotic Systems, Part I-Methodology, Part II-Applications," *Proceedings of 20th ASME Mechanisms Conference*, Orlando, FL. pp. 7~21.

Hogan, N., 1985, "Impedance Control : An Approach to Manipulation : Part Ⅰ, Ⅱ, Ⅲ," *ASME Journal of Dynamic Systems, Measurements and Control*, Vol. 107, pp. 1~24.

Kazerooni, H., et al., 1986, "Robust Compliant Motion for Manipulators, Part I:The Fundamental concept of Compliant Motion, Part II:Design Method," *IEEE Journal of Robotics and Automation*, Vol. RA-2, No. 2, pp. 83~92, 93~105.

McCallion, H., Alexander, K. V. and Pham, D.

T., 1980, "Aid for Automatic Assembly," *Ist Int' l. Conf. on Assembly Automation*, pp. 313~323.

Peshkin, M. A., 1990, "Programmed Compliance for Error Corrective Assembly," *IEEE Transactions on robotics and automation*, Vol. 6, No. 4, pp. 474~482.

Whitney, D. E., 1982, "Quasi-Static Assembly of Compliantly Supported Rigid Parts," *Journal of Dynamic Systems, Measurement, and Control*, Vol. 104, pp. 65~77.

Whitney, D. E., "Remote Center Compliance," 1986, in *Encyclopedia of Robotics System and Control*, edited by J.J. Diponio and Y. Hasegawa, published by Industrial Training Corporation, Vol. 2., pp. 1316~1324.

Whitney, D. E., 1987, "Historical Perspective and State of the Art in Robot Force Control," Int' l. Journal of Robotics Research, Vol. 6, No.1. pp. 3~14.

Yi, B. J. and Freeman, R.A., 1992, "Synthesis of Actively Adjustable Springs by Antagonistic Redundant Actuation," *Trans. ASME J. of Dynamic Systems, Measurement, and Control*, Vol. 114, Sep., pp. 454~461.

Appendix

The sensitivity matrices $\frac{\partial[G_\phi^u]}{\partial \boldsymbol{\phi}}$ and $\frac{\partial[G_\phi^u]^T}{\partial \boldsymbol{\phi}}$ in Eq. (38) can be obtained via the second order kinematic influence coefficient $[H_{\phi\phi}^u]$ (Yi and Freeman, 1992). That is, noting the definition of the second-order kinematic influence coefficient

$$H_{\phi_m\phi_n}^{u_p} = [H_{\phi\phi}^u]_{p:m:n} : = \frac{\partial}{\partial \phi_m}\left(\frac{\partial u_p}{\partial \phi_n}\right) \tag{A1}$$

and the definition of the sensitivity matrix $\frac{\partial[G_\phi^u]}{\partial \boldsymbol{\phi}}$

$$\left[\frac{\partial[G_\phi^u]}{\partial \boldsymbol{\phi}}\right]_{p:m:n} = \frac{\partial}{\partial \phi_p}\left(\frac{\partial u_m}{\partial \phi_n}\right) \tag{A2}$$

the relation between these two 3-dimensional matrices can be established directly by switching appropriate index, as below,

$$\left[\frac{\partial[G_\phi^u]}{\partial \boldsymbol{\phi}}\right]_{p:m:n} = [H_{\phi\phi}^u]_{m:p:n} \tag{A3}$$

Likewise,

$$\left[\frac{\partial[G_\phi^u]^T}{\partial \boldsymbol{\phi}}\right]_{p:m:n} = [H_{\phi\phi}^u]_{n:p:m}. \tag{A4}$$